Bioorganic Chemistry 107 (2021) 104630

Contents lists available at ScienceDirect

Bioorganic Chemistry

journal homepage: www.elsevier.com/locate/bioorg

Design and synthesis of methoxyphenyl- and coumarin-based chalcone derivatives as anti-inflammatory agents by inhibition of NO production and down-regulation of NF-κB in LPS-induced RAW264.7 macrophage cells

Soha H. Emam [a], Amr Sonousi [a,b,*], Eman O. Osman [a], Dukhyun Hwang [c], Gun-Do Kim [c], Rasha A. Hassan [a]

[a] Pharmaceutical Organic Chemistry Department, Faculty of Pharmacy, Cairo University, Cairo 11562, Egypt
[b] University of Hertfordshire Hosted by Global Academic Foundation, New Administrative Capital, Cairo, Egypt
[c] Department of Microbiology, College of Natural Sciences, Pukyong National University, Busan 48513, Republic of Korea

ARTICLE INFO

Keywords:
Chalcones
Anti-inflammatory
Nitric oxide inhibition
Nuclear factor kappa B
LPS-induced RAW264.7 macrophages
Molecular docking

ABSTRACT

Exaggerated inflammatory responses may cause serious and debilitating diseases such as acute lung injury and rheumatoid arthritis. Two series of chalcone derivatives were prepared as anti-inflammatory agents. Methoxylated phenyl-based chalcones **2a-l** and coumarin-based chalcones **3a-f** were synthesized and compared for their inhibition of COX-2 enzyme and nitric oxide production suppression. Methoxylated phenyl-based chalcones showed better inhibition to COX-2 enzyme and nitric oxide suppression than the coumarin-based chalcones. Among the 18 synthesized chalcone derivatives, compound **2f** exhibited the highest anti-inflammatory activity by inhibition of nitric oxide concentration in LPS-induced RAW264.7 macrophages (IC_{50} = 11.2 μM). The tested compound **2f** showed suppression of iNOS and COX-2 enzymes. Moreover, compound **2f** decreases in the expression of NF-κB and phosphorylated IκB in LPS-stimulated macrophages. Finally, docking studies suggested the inhibition of IKKβ as a mechanism of action and highlighted the importance of **2f** hydrophobic interactions.

1. Introduction

Inflammation is an immune response to irritants or infections that meant to help the body to eliminate these causes. However, in some cases, exaggerated inflammatory responses take place without any intruders to protect against or will stay even after the cause had been removed. This will damage the body as a result of the immune system attacking the body's own cells or tissues causing inflammatory diseases such as rheumatoid arthritis, rheumatic fever, asthma, and contributes to approximately 15% to 25% of human cancers [1]. Currently, non-steroidal anti-inflammatory drugs (NSAIDs) and steroids are the main treatment of these inflammatory disorders. The anti-inflammatory activity of NSAIDs is mainly due to the inhibition of cyclooxygenase (COX). COX is a crucial enzyme responsible for the synthesis of prostaglandins and messenger molecules in the process of inflammation [2]. Side effects, particularly gastric ulceration, and kidney toxicity have motivated researchers to focus on the design and the development of new anti-inflammatory drugs with different mechanisms of action to avoid these side effects [3–8].

Macrophages play an important role in the inflammation process. In macrophages, irritants as lipopolysaccharides (LPS) originated mainly from Gram-negative bacteria trigger downstream signal transduction such as activation of the inhibitor of κB kinase (IKK) proteins that lead to nuclear factor κB (NF-κB) activation which up-regulate the expression of a series of inflammatory genes resulting in synthesis of inducible enzymes such as cyclooxygenase-2 (COX-2) and inducible nitric oxide synthase (iNOS) [9]. iNOS converts L-arginine into L-citrulline producing nitric oxide (NO) in the process (Fig. 1). NO is a short-lived bioactive molecule released into the endothelial cells that participate in the inflammation disorders and large amounts of NO may lead to tissue damage. Excessive NO production by activated macrophages has been observed in many inflammatory diseases [10]. Therefore, development of potent and selective inhibitors of NO would be valuable for potential therapeutic use.

Chalcones (benzalacetophenone) consist of enone system enclosed by two rings. Chalcones are widely present naturally in plants (including fruits, vegetables, spices, and tea) especially in the flavonoid family where they are used as a biosynthetic precursor [11]. Literature survey

* Corresponding author.
E-mail address: amr.motawi@pharma.cu.edu.eg (A. Sonousi).

https://doi.org/10.1016/j.bioorg.2021.104630
Received 30 September 2020; Received in revised form 1 January 2021; Accepted 2 January 2021
Available online 7 January 2021

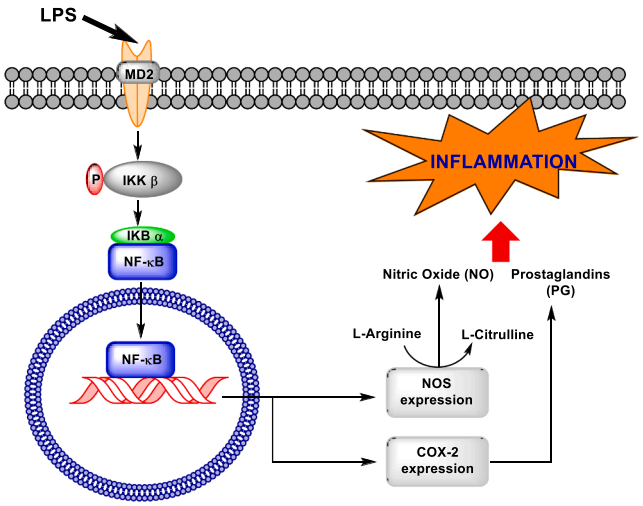

Fig. 1. A schematic diagram showing the role of IKK β, IκB and NF-κB in inducing the expression of nitric oxide synthase (NOS) and COX-2 enzymes which lead to inflammation response.

has shown that naturally occurring chalcones are of great chemical and pharmacological interest, as they have excellent anticancer, anti-inflammatory, antibacterial, and antihyperlipidemic activity [12–18]. Also, they inhibit NO production, iNOS and COX-2 protein expression in lipopolysaccharide (LPS) stimulated cells [19,20]. Chalcone derivatives as curcumin have been extensively reported to exhibit their potential in the therapy of inflammatory and immune diseases [21–24]. Moreover, coumarins have been reported to possess anti-inflammatory activities [25–28], even the simple coumarin umbelliferone exhibited a significant anti-edema effect in carrageenan-induced rat paw edema assay (Fig. 2) [29].

In this study, a series of di- and tri methoxyphenyl chalcones as well as coumarin-based chalcones were designed and synthesized. We evaluated the inhibitory effect of the 18 synthetic chalcone derivatives against COX-1 and COX-2 enzymes. All derivatives were tested for their inhibition of nitric oxide (NO) production in LPS-stimulated macrophages. The Structure-activity relationship was discussed to determine the relationship between the structures of synthesized compounds and their pharmacological effects. Further, the most active chalcone was selected for the study of anti-inflammatory mechanism at the transcriptional level. Finally, docking studies were done to rationalize the biological activity.

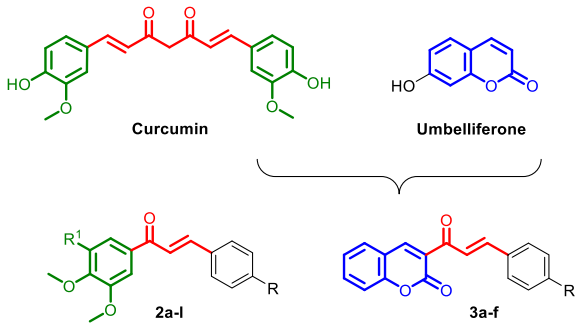

Fig. 2. A diagram showing the common structural features between the designed targets and both the lead compounds curcumin and umbelliferone.

2. Results and discussion

2.1. Chemistry

New methoxyphenyl chalcones **2a-l**, and coumarin chalcones **3a-f** were synthesized. The synthetic procedures to obtain the target compounds are illustrated in Scheme 1 and 2. Accordingly, aryloxybenzaldehydes **1a-c** and dialkylaminobenzaldehydes **1d-f** were synthesized *via* nucleophilic aromatic substitution reaction of 4-fluorobenzaldehyde as the starting compound with substituted phenols or secondary amines in the presence of K_2CO_3 in DMF according to the methods reported in the literature [30,31].

As shown in Scheme 1, A series of 1,3-diaryl-2-propen-l-ones **2a-l** were obtained in good to excellent yields (80–91%) by using Claisen-Schmidt condensation of 3,4-dimethoxyacetophenone or 3,4,5-trimethoxyacetophenone with different aryloxybenzaldehydes **1a-c** and dialkylaminobenzaldehydes **1d-f** in ethanol containing potassium hydroxide as a catalyst [32,33].

The route followed for the preparation of coumarin-chalcone derivatives **3a-f** is illustrated in Scheme 2. The starting material 3-acetyl-2*H*-chromen-2-one was obtained *via* Knoevenagel reaction by reacting salicylaldehyde and ethylacetoacetate in the presence of catalytic amount of piperidine according to the procedure reported in the literature [34]. Claisen-Schmidt condensation of 3-acetyl-2*H*-chromen-2-one with aryloxybenzaldehydes **1a-c** and dialkylaminobenzaldehydes **1d-f** in refluxing ethanol containing piperidine as a catalyst yielded the desired target chalcones **3a-f** according to a previously reported method [35].

All the newly synthesized compounds were characterized by ^{1}HNMR, ^{13}CNMR, IR and elemental analysis. ^{1}HNMR, ^{13}CNMR spectra are provided in the supplementary materials. The IR spectra of chalcones **2a-l** showed the existence of a carbonyl group conjugated with the olefinic bond CH═CH, which appeared at a lower wavenumber in the range of 1643–1654 cm^{-1}. The formation of CH═CH—CO group was also confirmed in ^{1}HNMR by the appearance of two doublet signals at δ 7.68–7.95 ppm and δ 7.39–7.75 ppm. The coupling constant of the olefinic protons confirmed the *trans* configuration (J value = 15.6 Hz). The existence of methoxy groups was confirmed by singlet signals at the range of δ 3.76–3.96 ppm. In compound **2g**, the characteristic signals of the piperidine ring were observed in the range of δ 1.60–3.30 ppm. Moreover, the ^{1}HNMR spectra of **2i** and **2L** showed a singlet signal at δ 2.22 ppm due to NCH_3 and two triplets in the range of δ 2.44–3.29 ppm of piperazine ring moiety. ^{13}C NMR spectra of chalcones **2a-l** showed the presence of carbonyl carbon at δ 187.5–188.8 ppm along with the olefinic carbons at the ranges of δ 142.0–144.6 and δ 121.3–124.7 ppm. Moreover, compound **2g** showed three signals of piperidine ring carbons at δ 24.3, 25.4 and 49.1 ppm while piperazine ring appeared as two signals around δ 46.0 and 47.0 ppm in ^{13}C NMR spectra of chalcones **2i** and **2L**.

In coumarin chalcones **3a-f**, IR spectra showed two prominent bands in the range of 1651 and 1720 cm^{-1} corresponding to carbonyl group of chalcone moiety and coumarin moiety respectively. In the ^{1}HNMR spectra, the signal of the proton at position 4 of the chromene ring appeared as a singlet around δ 8.60 ppm. Compound **3d** showed the characteristic signals of the piperidine ring at δ 1.58 as 6H and a multiplet of 4H at 3.44–3.30 ppm appeared after treatment with D_2O. Additionally, two triplet signals of morpholine ring system with integration of 4 protons each, appeared at δ 3.27 ppm and δ 3.74 ppm in the ^{1}HNMR spectrum of compounds **3e.** Moreover, the ^{1}HNMR spectrum of **3f** showed a singlet signal at δ 2.22 ppm due to NCH_3 and two triplets at δ 2.44 and 3.31 ppm of piperazine ring moiety. ^{13}C NMR spectra showed the olefinic carbons at the range δ 143.4–145.6 and δ 123.5–124.7 ppm along with the presence of two carbonyl carbons in the range of δ 187.1–189.1 ppm and δ 158.8–164.4 ppm due to chalcone and coumarin lactone carbonyl groups, respectively. Moreover, three signals of piperidine ring system appeared at δ 24.4, 25.3 and 48.3 ppm in the

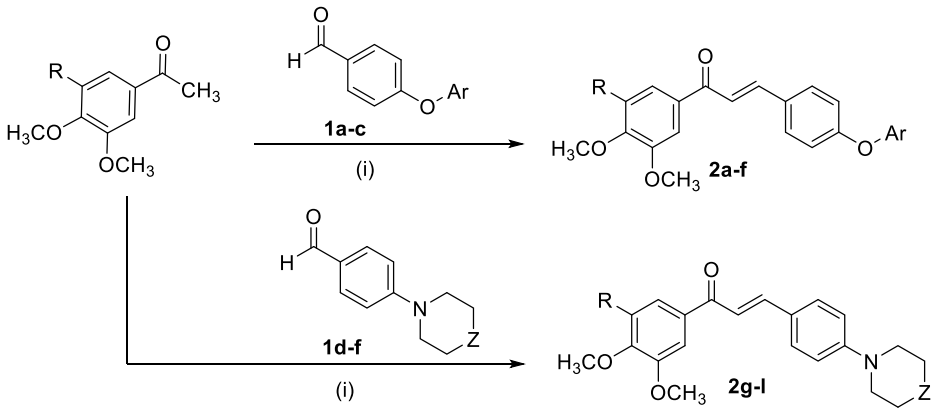

1a: Ar = 4-ClC_6H_4- **1b**: Ar = 4-BrC_6H_4- **1c**: Ar = 4-$OCH_3C_6H_4$-
1d: Z = CH_2 **1e**: Z = O **1f**: Z = NCH_3

2a: R = H; Ar = 4-ClC_6H_4-
2b: R = H; Ar = 4-BrC_6H_4-
2c: R = H; Ar = 4-$OCH_3C_6H_4$-
2d: R = OCH_3; Ar = 4-ClC_6H_4-
2e: R = OCH_3; Ar = 4-BrC_6H_4-
2f: R = OCH_3; Ar = 4-$OCH_3C_6H_4$-
2g: R = H; Z = CH_2
2h: R = H; Z = O
2i: R = H; Z = NCH_3
2j: R = OCH_3; Z = CH_2
2k: R = OCH_3; Z = O
2l: R = OCH_3; Z=NCH_3

Scheme 1. Synthesis of methoxyphenyl chalcones 2a-l starting from 3,4-dimethoxyacetophenone and 3,4,5-trimethoxyacetrophenone: i) 40% KOH, 95% ethanol, 0 °C.

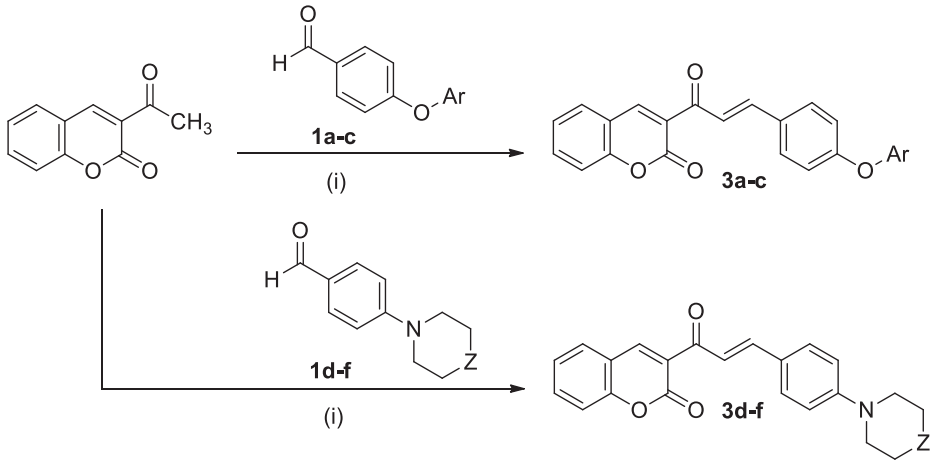

3a: Ar = 4-ClC_6H_4- **3b**: Ar = 4-BrC_6H_4- **3c**: Ar = 4-$OCH_3C_6H_4$-
3d: Z = CH_2 **3e**: Z = O **3f**: Z = NCH_3

Scheme 2. Synthesis of coumarin chalcones 3a-f starting from 3-acetylcoumarin: i) piperidine, 95% ethanol, reflux 6 h.

^{13}CNMR spectrum of **3d** while two signals of morpholine in compound **3e** appeared at δ 47.41 and 66.3 ppm. Additionally, the ^{13}C NMR spectrum of **3f** showed the characteristic signals of piperazine ring at δ 46.7 and 47.1 ppm.

2.2. Biological results

2.2.1. Inhibitory effect (IC_{50}) of the synthesized chalcones on COX-1 and COX-2 enzymes

All compounds were screened for their *in vitro* inhibition of COX-1 and COX-2 enzymes. Generally, the synthesized compounds showed a less inhibitory effect towards the inducible COX-2 enzyme compared to the reference drugs (celecoxib and rofecoxib). Compounds **2a-f** bearing phenoxy derivatives have a significant better activity than compounds **2g-l** with piperidine, morpholine or piperazine rings. Compounds **2a-e** demonstrated a comparable result as celecoxib and better activity than indomethacin (Fig. 3A). The same argument is true in the coumarin-based chalcones where **3a-c** showed better inhibitory activities than **3d-f**. COX-1 enzyme is a constitutive "housekeeping" where its excessive inhibition may cause GI ulcers and side effects accompanied by

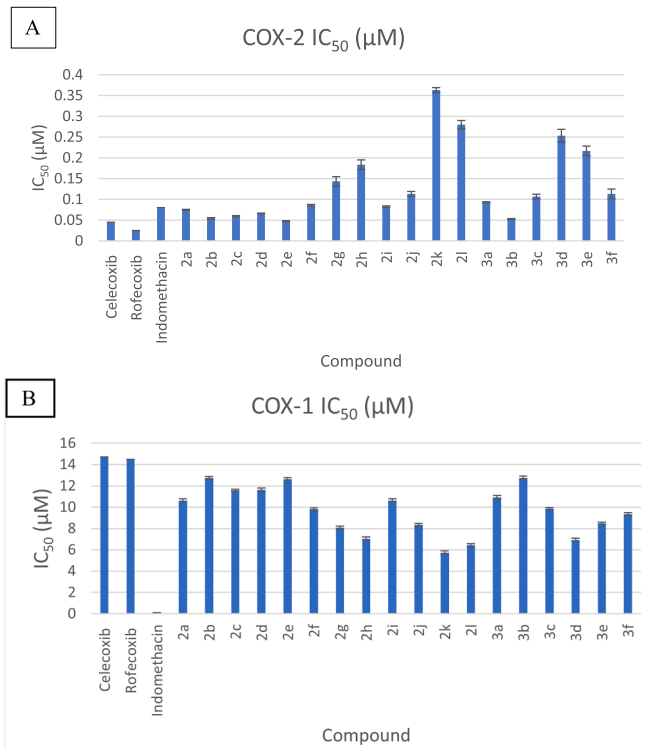

Fig. 3. A bar diagram showing the *in vitro* IC_{50} inhibitory assay of the target compounds on **A)** COX-2 and **B)** COX-1 enzymes.

indomethacin and other nonselective COX inhibitors [36,37]. All target compounds showed weak inhibitory activity to the constitutive COX-1 enzyme compared to indomethacin and hence less prone to the side effects of COX-1 inhibition. Compounds with 4-bromophenoxy group **2b**, **2e** and **3e** were the best among the synthesized derivatives and demonstrated a comparable activity to the selective celecoxib and rofecoxob (Fig. 3B).

2.2.2. Inhibition of NO production on LPS-induced RAW264.7 macrophage cells

Inhibition of nitric oxide production is an important pathway to treat various inflammatory diseases [38]. High amount of nitric oxide is one of the causes that lead to tissue damage in many inflammatory disorders as rheumatoid arthritis where large amount of nitric oxide is liberated from the macrophages [39]. The target compounds were tested for their ability to decrease nitric oxide concentration in LPS-activated RAW 264.7 macrophages. The macrophages were treated with the target compounds and LPS (1 μg/mL) for 24 h. The nitric oxide (NO) production was indirectly analyzed by measuring the nitrite concentration based on the Griess reaction [40]. As an initial screening, compounds at concentrations of 100 μM and 50 μM were used (Fig. 4A). The dimethoxyphenyl chalcone derivatives were better than their trimethoxyphenyl chalcones counterpart. In general, the coumarin-based chalcone derivatives (with exception to **3e**) were less active than the di- and trimethoxyphenyl-based chalcones. Upon decreasing the concentrations of the tested compounds to 25 μM and 5 μM, **3d** showed the highest inhibition of NO conc. but with some cytotoxicity, the cell morphology of the lymphocytes was changed, and some cells were died, and hence **3d** was excluded from further analysis. The 4-methoxyphenoxy group carrying compounds (**2f** and **3c**) were the best in NO inhibition at 25 μM (Fig. 4B). All target compounds that were able to decrease the NO conc. below 3 μM in the LPS-induced RAW264.7 cells at conc. 25 μM were retested again at different concentrations ranges from 5 μM to 20 μM (Fig. 5). Among the tested compounds, **2f** showed the best NO inhibition profile with 87% inhibitory activity on NO production at 20 μM and therefore was chosen for further investigations.

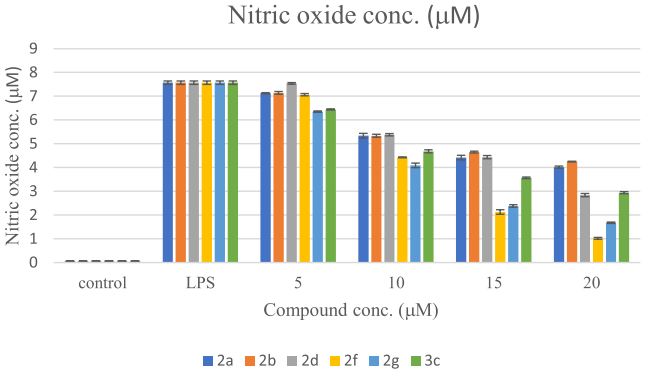

Fig. 5. A bar diagram representation showing the activity in decreasing the nitric oxide conc in the LPS-induced RAW264.7 macrophage cells at conc. of 5 μM, 10 μM, 15 μM and 20 μM of the most active candidates.

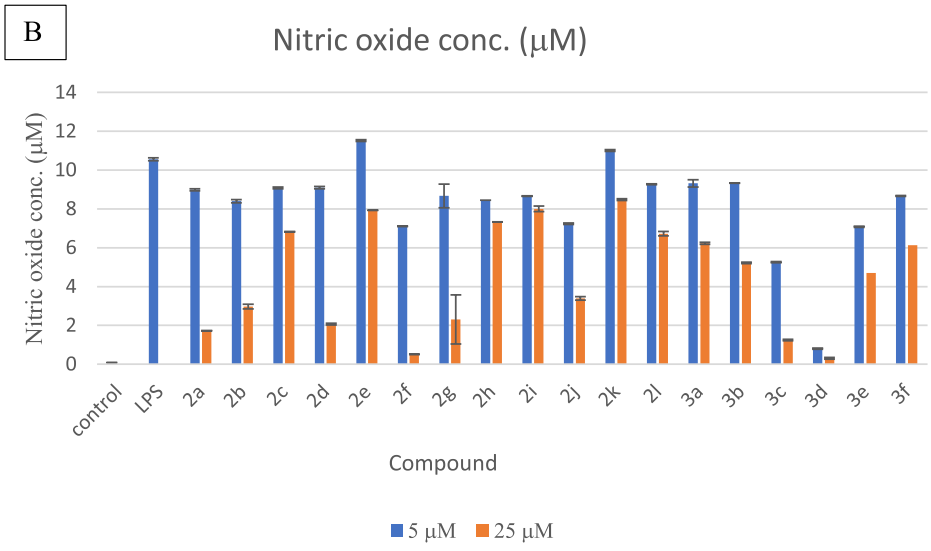

Fig. 4. A bar diagram representation showing the inhibition of the nitric oxide conc in LPS-induced RAW264.7 macrophage cells A) at conc. of 50 μM and 100 μM and B) at conc. of 5 μM and 25 μM of the target compounds.

2.2.3. Effects of 2f on cell viability

Before further studies on compound **2f**, the effect of **2f** on cell viability was tested [41]. The anti-inflammatory effects of **2f** was examined on RAW264.7 cells by MTT (3-(4,5-dimethylthiazol-2-yl)-2,5-diphenyltetrazolium bromide) assay (Fig. 6). The level of MTT dye is a measure of the cellular metabolic activity. The test is used to determine the cytotoxicity potential of the medicinal compounds on the cells. As shown in Fig. 6, **2f** did not affect cell viability of RAW264.7 cells even at 20 μM.

2.2.4. Inhibition of NO, iNOS and COX-2 expression by 2f on LPS-induced RAW264.7 cells

Based on the absence of cytotoxicity of **2f**, the response of NO inhibition at different concentrations of **2f** was measured on LPS-induced RAW264.7 cells with IC_{50} = 11.2 μM. Compounds **2f** exhibited stronger inhibition than quercetin (IC_{50} = 26.8 μM), which was reported to inhibit NO production from LPS activated RAW 264.7 cells [42,43]. we examined the effects of **2f** on iNOS and COX-2 expression by using Western blot analysis [44]. Compound **2f** was incubated with RAW264.7 cells then collected and lysed with an ice-cold lysis buffer. The enzymes were blocked using suitable antibodies and detected by ECL solution®. Fig. 7 showed that the nitrite conc. was decreased with a dose dependent manner of **2f.** Compound **2f** highly inhibited the iNOS and COX-2 expression especially at 20 μM in LPS-induced RAW264.7 cells.

2.2.5. Inhibitory effects of NF-κB pathway by 2f on LPS-stimulated RAW264.7 cells

Cytokine expression, apoptosis regulation and cell proliferation are highly dependent on the transcription factor NF-κB which plays a crucial role in the inflammatory response's regulation [45]. NF-κB activation triggers the transcription of iNOS, COX-2 enzymes that are important pathways of inflammatory response. The effect of compound **2f** in suppressing the activation of NF-κB was investigated by measuring its phosphorylated forms in the LPS-induced RAW264.7 cells using Western blot analysis. Before adding LPS as an inflammatory stimulant, NF-κB was bound with the inhibitory protein of the IκB family in the cytoplasm and hence rendered inactive. When the stimulation is triggered, IκB proteins are phosphorylated by IκB kinase then NF-κB is translocated into the nucleus [46]. As shown in Fig. 8, **2f** considerably decreased phosphorylation of IκB as well as NF-κB in a dose dependent manner which proves the ability of **2f** to decrease inflammatory response from the transcription level.

2.2.6. Structure-activity relationship (SAR)

Eighteen chalcone compounds were synthesized and evaluated for their anti-inflammatory through COX-2 inhibition as well as their ability to decrease the concentration of nitric oxide in LPS induced cells.

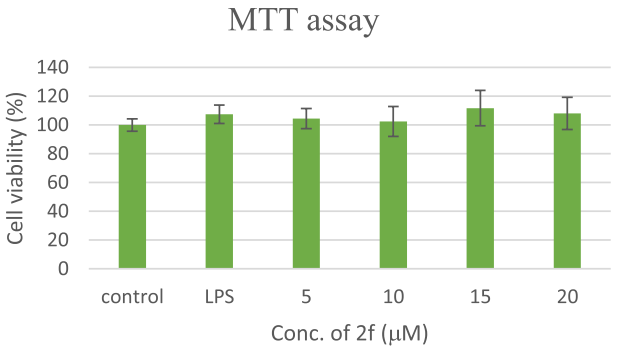

Fig. 6. RAW264.7 cells were stimulated with LPS (1 μg/mL) for 24 h. The cell viability assay of compound **2f** was performed in triplicates by WST-1® (Daeil Lab Service, Gyeonggi, Korea) and the results are presented as the mean ± standard error.

Substitution of R^1 with phenoxy derivative will have more potent anti COX-2 activity compared to disubstituted amines attached in the same position (Fig. 9). Substitution of R^4 with Br increases the COX selectivity. Di- and trimethoxy phenyl groups at the R position favor the nitric oxide inhibition with trimethoxy more active the dimethoxy derivative at low concentrations. On the other hand, coumarin ring at position R causes less nitric oxide inhibition.

2.3. Docking studies

In the search for the potential mechanism of the compounds in inhibition of NF-κB pathway, compounds (**2a**, **2f**, **2g** and **3c**) that were able to decrease the NO conc. below 3 μM in the LPS-induced RAW264.7 cells at conc. 25 μM were docked to the crystal structure of the IκB kinase (IKK β) (PDB code: 4KIK) [47] using MOE molecular docking software. The IκB kinase enzyme complex is part of the upstream NF-κB signal transduction cascade. IκB kinase is an enzyme complex that phosphorylate IκB proteins which activates NF-κB and thereby propagating the cellular response to inflammation. The docking scores as well as Lipinski parameters are shown in Table 1. Compound **2f** showed the best docking score (−7.75 kcal/mol) with no violations in Lipinski parameters compared to compounds **2b** and **3c** with logP more than 5. As a result, it can be concluded that the **2f** possess property of drug-likeness. Molecular docking study revealed that compound **2f** fits into the hydrophobic pocket of IκB kinase with docking score = −7.75 $kcalmol^{-1}$ (Fig. 10). It can be observed that the trimethoxy phenyl group was embedded into a hydrophobic cleft formed by Tyr169, Gly184, and Glu 149 residues. The phenoxy phenyl group was embedded into a hydrophobic cleft formed by Ile-165, Val-29, Tyr-98, Leu-21, Cys-99, Gly-102, Met-96, Val-74, Val-152, and Gly-101 amino acids. The phenoxyphenyl of **2f** forms H-π stacking with the Val-152, Val-29 and Ile-165 that stabilize the binding conformation. In summary, important hydrophobic interactions were clarified as a suggestive mechanism of **2f** and IKKβ interaction.

3. Conclusion

Two series of chalcones either methoxylated phenyl chalcones or coumarin based chalcones were designed from curcumin and umbelliferone and synthesized. All compounds were tested for their anti-inflammatory. Phenoxy derivatives showed higher anti COX-2 activity compared to disubstituted amines. Moreover, di- and trimethoxy phenyl groups favor the nitric oxide inhibition with trimethoxy more active than the dimethoxy derivative at low concentrations. On the other hand, the coumarin ring exhibited less nitric oxide inhibition. Among the 18 synthesized chalcone derivatives, compound **2f** displayed the strongest anti-inflammatory activity by inhibition of NO (IC_{50} = 11.2 μM). The tested compound **2f** showed suppression of iNOS and COX-2 which was done by decreasing the expression NF-κB in LPS-stimulated macrophages. Finally, docking studies suggested the mechanism of inhibition of IKKβ enzyme and highlighted the importance of **2f** hydrophobic interactions.

4. Experimental

4.1. Chemistry

4.1.1. General

Melting points were obtained on a Griffin apparatus and were uncorrected. Microanalyses for C, H and N were carried out at the Regional Center for Mycology and Biotechnology, Faculty of Pharmacy, Al-Azhar University. IR spectra were recorded on Shimadzu IR 435 spectrophotometer (Shimadzu Corp., Kyoto, Japan) Faculty of Pharmacy, Cairo University, Cairo, Egypt and values were represented in cm^{-1}. ^1H NMR spectra were carried out on Bruker 400 MHz (Bruker Corp., Billerica, MA, USA) spectrophotometer, Faculty of Pharmacy, Cairo University, Cairo, Egypt. The chemical shifts were recorded in ppm on δ scale,

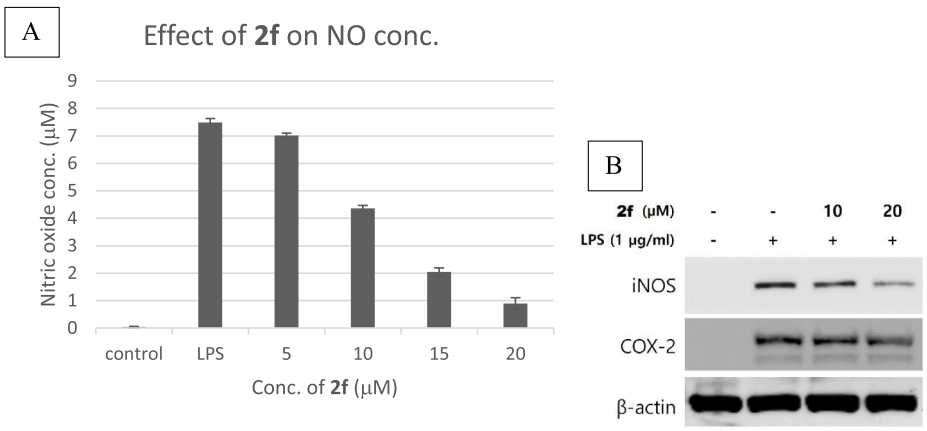

Fig. 7. Effects of **2f** on iNOS and COX-2 expression in LPS-induced RAW264.7 cells. Cells were pretreated with the designated concentration for 2 h and induced with LPS (1 μg/mL) for 24 h. (**A**) NO production was determined at different concentrations of **2f**; (**B**) iNOS and COX-2 expressions were determined by Western blot analysis. β-Actin was used as an internal control. Data means ± standard errors of the mean (SEM) from three independent experiments (see supporting information).

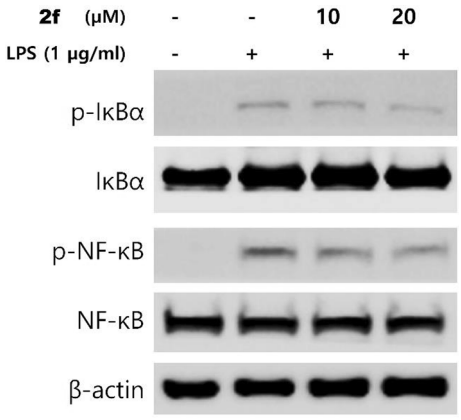

Fig. 8. Effects of **2f** on phosphorylation of either NF-κB or IκBα, and NF-κB translocation in LPS-stimulated RAW264.7 cells. Cells were pretreated with the designated concentration of **2f** for 2 h and induced with LPS (1 μg/mL). Cell lysates were subjected to Western blot analysis using antibodies against p-IκBα, IκBα, p-NF-κB and NF-κB. β -Actin was used as an internal control. Data means ± standard errors of the mean (SEM) from three independent experiments (see supporting information).

coupling constants (*J*) were given in Hz and peak multiplicities are designed as follows: s, singlet; d, doublet; dd, doublet of doublet; t, triplet; m, multiplet ^{13}C NMR spectra were carried out on Bruker 100 MHz spectrophotometer, Faculty of Pharmacy, Cairo University, Cairo, Egypt. Progress of the reactions were monitored by TLC using precoated aluminum sheet silica gel MERCK 60F 254 and was visualized by UV lamp.

The original NMR spectra of the investigated compounds are provided as supporting information. *4-(4-substitutedphenoxy)benzaldehyde* (**1a-c**) [31], *4-morpholinobenzaldehyde* (**1d**) [30], 4-(piperidin-1-yl) benzaldehyde (**1e**) [30], 4-(4-methylpiperazin-1-yl)benzaldehyde (**1f**) [48] and *3-acetyl-2H-chromen-2-one* [34] were synthesized according to

Table 1
The docking score and Lipinski parameters of compounds 2b, 2f, 2g and 3c.

Compound number	Docking score (kcal/mol)	HBA (≤10)	HBD (≤5)	LogP (−4.0–5)	PSA (0–150) Å^2
2b	−7.07	4	0	6.1	44.7
2f	−7.75	6	0	5.0	63.2
2g	−7.06	4	0	4.6	38.7
3c	−7.25	5	0	5.6	61.8

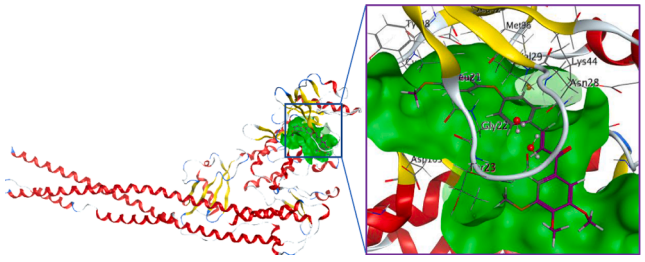

Fig. 10. Molecular docking of compound **2f** to the hydrophobic cavity of IKKβ (PDB: 4KIK).

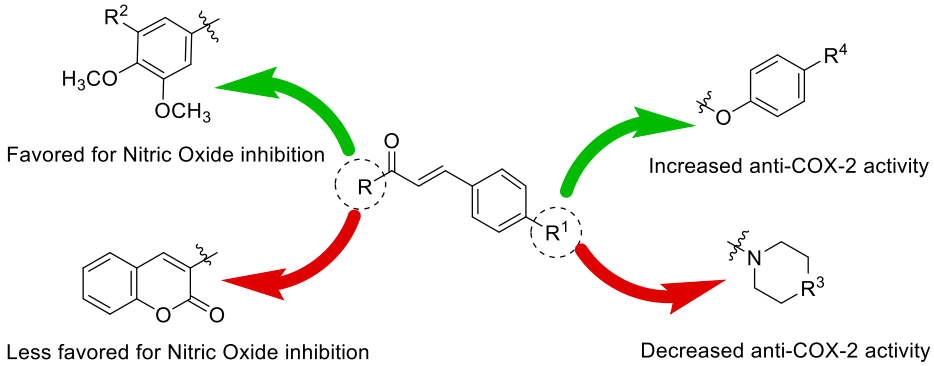

Fig. 9. Structure-activity relationship (SAR) of the synthesized chalcone derivatives.

the reported procedures. Chalcones *(E)-1-(3,4-dimethoxyphenyl)-3-(4-morpholinophenyl)prop-2-en-1-one* **(2h)** [49], *(E)-3-(4-(piperidin-1-yl) phenyl)-1-(3,4,5-trimethoxyphenyl)prop-2-en-1-one* **(2j)** [50] and *(E)-3-(4-morpholinophenyl)-1-(3,4,5-trimethoxyphenyl)prop-2-en-1-one* ***(2k)*** [49] were prepared in the mentioned references.

4.1.2. General procedure for the preparation of methoxyphenyl chalcones ***2a-l***

To an ice cooled, stirred solution of the selected aldehyde (0.01 mol) (**1a-f**) and 3,4-dimethoxyacetophenone or 3,4,5-trimethoxyacetophenone (0.01 mol) in 95% ethanol, was added portion wise 40% aqueous KOH solution. Stirring was continued at 0 °C for 6 h. Solid product was filtered and washed with 3% aqueous HCl and crystallized from ethanol.

3-(4-(4-chlorophenoxy)phenyl)-1-(3,4-dimethoxyphenyl)prop-2-en-1-one **(2a):** Yellow solid: 90% yield; mp 146–148 °C; IR (KBr, cm^{-1}) 3066 (CH aromatic), 2970, 2935 (CH aliphatic), 1651 (C═O), 1597, 1573 (C═C); ^{1}H NMR (400 MHz, DMSO-d_6) δ 7.95–7.87 (m, 4H, ArH + CH═CH—CO), 7.71 (d, J = 15.6 Hz, 1H, CH═CH—CO), 7.61 (d, J = 2.0 Hz, 1H, ArH), 7.50–7.46 (m, 2H, ArH), 7.14–7.07 (m, 5H, ArH), 3.88 (s, 3H, OCH_3), 3.86 (s, 3H, OCH_3); ^{13}C NMR (100 MHz, DMSO-d_6) δ:187.7, 158.7, 155.2, 153.6, 149.2, 142.7, 131.3, 131.0, 130.8, 130.5, 128.3, 123.7, 121.5, 121.3, 119.0, 111.3, 111.2, 56.2, 56.0; Anal. Calcd for $C_{23}H_{19}ClO_4$ (394.85): C, 69.96; H, 4.85; found C, 70.18; H, 5.07.

3-(4-(4-bromophenoxy)phenyl)-1-(3,4-dimethoxyphenyl)prop-2-en-1-one **(2b):** Yellow solid: 91% yield; mp 184–186 °C; IR (KBr, cm^{-1}) 3062 (CH aromatic), 2966, 2935 (CH aliphatic), 1651 (C═O), 1597, 1570 (C═C); ^{1}H NMR (400 MHz, DMSO-d_6) δ 7.96–7.88 (m, 4H, ArH + CH═CH—CO), 7.71 (d, J = 15.6 Hz, 1H, CH═CH—CO), 7.62–7.58 (m, 3H, ArH), 7.12–7.04 (m, 5H, ArH), 3.88 (s, 3H, OCH_3), 3.87 (s, 3H, OCH_3); ^{13}C NMR (100 MHz, DMSO-d_6) δ:187.7, 158.6, 155.7, 153.6, 149.2, 142.7, 133.4, 131.3, 131.0, 130.8, 123.8, 121.7, 121.5, 119.1, 116.2, 111.3, 111.1, 56.2, 56.0; Anal. Calcd for $C_{23}H_{19}BrO_4$ (439.30): C, 62.88; H, 4.36; found C, 63.15; H, 4.49.

1-(3,4-dimethoxyphenyl)-3-(4-(4-methoxyphenoxy)phenyl)prop-2-en-1-one **(2c):** Yellow solid: 81% yield; mp 122–124 °C; IR (KBr, cm^{-1}) 3078 (CH aromatic), 2943, 2912 (CH aliphatic), 1651 (C═O), 1590, 1566 (C═C); ^{1}H NMR (400 MHz, DMSO-d_6) δ 7.90–7.83 (m, 4H, ArH + CH═CH—CO), 7.69 (d, J = 15.6 Hz, 1H, CH═CH—CO), 7.60 (d, J = 2.0 Hz, 1H, ArH), 7.12–7.06 (m, 3H, ArH), 7.03–7.00 (m, 2H, ArH), 6.99–6.95 (m, 2H, ArH), 3.88 (s, 3H, OCH_3), 3.86 (s, 3H, OCH_3), 3.78 (s, 3H, OCH_3); ^{13}C NMR (100 MHz, DMSO-d_6) δ:187.7, 160.5, 156.5, 153.6, 149.2, 148.9, 143.0, 131.2, 131.0, 129.6, 123.7, 121.7, 120.9, 117.5, 115.6, 111.3, 111.1, 56.2, 56.0, 55.89; Anal. Calcd for $C_{24}H_{22}O_5$ (390.43): C, 73.83; H, 5.68, found C, 73.60; H, 5.85.

3-(4-(4-chlorophenoxy)phenyl)-1-(3,4,5-trimethoxyphenyl)prop-2-en-1-one **(2d):** Yellow solid: 89% yield; mp 160–162 °C; IR (KBr, cm^{-1}) 3093 (CH aromatic), 2993, 2935 (CH aliphatic), 1654 (C═O), 1570 (C═C); ^{1}H NMR (400 MHz, DMSO-d_6) δ 7.97–7.95 (m, 2H, ArH), 7.89 (d, J = 15.6 Hz, 1H, CH═CH—CO), 7.75 (d, J = 15.6 Hz, 1H, CH═CH—CO), 7.50–7.46 (m, 2H, ArH), 7.43 (s, 2H, ArH), 7.15–7.08 (m, 4H, ArH), 3.91 (s, 6H, 2 OCH_3), 3.77 (s, 3H, OCH_3); ^{13}C NMR (100 MHz, DMSO-d_6) δ:188.2, , 158.8, 155.2, 153.3, , 143.5, 142.4, 133.5, 131.5, 130.7, 130.5, 128.3, 121.5, 121.3, 119.0, 106.6, , 60.6, 56.6; Anal. Calcd for $C_{24}H_{21}ClO_5$ (424.87): C, 67.85; H, 4.98, found, C, 67.98; H, 5.24.

3-(4-(4-bromophenoxy)phenyl)-1-(3,4,5-trimethoxyphenyl)prop-2-en-1-one **(2e):** Yellow solid: 89% yield; mp 190–192 °C; IR (KBr, cm^{-1}) 3088 (CH aromatic), 2997, 2935 (CH aliphatic), 1654 (C═O), 1570 (C═C); ^{1}H NMR (400 MHz, DMSO-d_6) δ 7.99–7.96 (m, 2H, ArH), 7.89 (d, J = 15.6 Hz, 1H, CH═CH—CO), 7.75 (d, J = 15.6 Hz, 1H, CH═CH—CO), 7.63–7.59 (m, 2H, ArH), 7.43 (s, 2H, ArH), 7.13–7.05 (m, 4H, ArH), 3.91 (s, 6H, 2 OCH_3), 3.78 (s, 3H, OCH_3); ^{13}C NMR (100 MHz, DMSO-d_6) δ:188.2, 158.7, 155.7, 153.3, 143.0, 142.4, 133.5, 133.4, 131.5, 130.7, 121.7, 121.5, 119.1, 116.2, 106.6, 60.6, 56.6; Anal. Calcd for $C_{24}H_{21}BrO_5$ (469.32): C, 61.42; H, 4.51, found C, 61.70; H, 4.38.

3-(4-(4-methoxyphenoxy)phenyl)-1-(3,4,5-trimethoxyphenyl)prop-2-en-1-one **(2f):** Yellow solid: 90% yield; mp 138–140 °C; IR (KBr, cm^{-1}) 3066 (CH aromatic), 2947, 2932 (CH aliphatic), 1654 (C═O), 1573 (C═C); ^{1}H NMR (400 MHz, DMSO-d_6) δ 7.92–7.88 (m, 2H, ArH), 7.85 (d, J = 15.6 Hz, 1H, CH═CH—CO), 7.72 (d, J = 15.6 Hz, 1H, CH═CH—CO), 7.42 (s, 2H, ArH), 7.10–7.06 (m, 2H, ArH), 7.02–6.99 (m, 2H, ArH), 6.98–6.96 (m, 2H, ArH), 3.90 (s, 6H, 2 OCH_3), 3.78 (s, 3H, OCH_3), 3.77 (s, 3H, OCH_3); ^{13}C NMR (100 MHz, DMSO-d_6) δ:188.2 (C═O), 160.6, 156.5, 153.3, 149.9, 143.7, 142.3, 133.5, 131.4, 129.5, 121.6, 120.9, 117.4, 115.6, 106.5, 106.2, 60.6, 56.6, 55.8; Anal. Calcd for $C_{25}H_{24}O_6$ (420.45): C, 71.41; H, 5.75, found C, 71.68; H, 5.94.

1-(3,4-dimethoxyphenyl)-3-(4-(piperidin-1-yl)phenyl)prop-2-en-1-one **(2g):** Yellow oil: 84% yield; IR (KBr, cm^{-1}) 3085 (CH aromatic), 2960, 2939 (CH aliphatic), 1654 (C═O), 1580 (C═C); ^{1}H NMR (400 MHz, $CDCl_3$) δ 7.78 (d, J = 15.6 Hz, 1H, CH═CH—CO), 7.68 (dd, J = 2.0, 8.4 Hz, 1H, ArH), 7.62 (d, J = 2.0 Hz, 1H, ArH), 7.54 (d, J = 8.4 Hz, 1H, ArH), 7.39 (d, J = 15.6 Hz, 1H, CH═CH—CO), 6.93–6.88 (m, 3H, ArH), 3.96 (s, 3H, OCH_3), 3.95 (s, 3H, OCH_3), 3.30 (t, J = 5.2 Hz, 4H, $2CH_2$ piperidine), 1.72–1.66 (m, 4H, $2CH_2$ piperidine), 1.65–1.60 (m, 2H, CH_2 piperidine); ^{13}C NMR (100 MHz, $CDCl_3$) δ:188.8, 153.0, 152.8, 149.1, 144.6, 131.9, 130.1, 124.6, 122.6, 117.4, 114.9, 110.8, 109.9, 56.1, 56.0, 49.1, 25.4, 24.3; Anal. Calcd for $C_{22}H_{25}NO_3$ (351.44): C, 75.19; H, 7.17; N, 3.99, found C, 75.02; H, 7.39; N, 4.25.

1-(3,4-dimethoxyphenyl)-3-(4-(4-methylpiperazin-1-yl)phenyl)prop-2-en-1-one **(2i):** Yellow solid: 80% yield; mp 173–175 °C; IR (KBr, cm^{-1}) 3082 (CH aromatic), 2962, 2939 (CH aliphatic), 1643 (C═O), 1589 (C═C); ^{1}H NMR (400 MHz, DMSO-d_6) δ 7.87 (dd, J = 2.0, 8.4 Hz, 1H, ArH), 7.75–7.71 (m, 3H, ArH + CH═CH—CO), 7.64 (d, J = 15.6 Hz, 1H, CH═CH—CO), 7.60 (d, J = 2.0 Hz, 1H, ArH), 7.09 (d, J = 8.4 Hz, 1H, ArH), 6.98 (d, J = 8.4 Hz, 2H, ArH), 3.87 (s, 3H, OCH_3), 3.86 (s, 3H, OCH_3), 3.28 (t, J = 4.8 Hz, 4H, $2CH_2$ piperazine), 2.44 (t, J = 4.8 Hz, 4H, $2CH_2$ piperazine), 2.22 (s, 3H, NCH_3); ^{13}C NMR (100 MHz, DMSO-d_6) δ:187.5, 153.3, 152.8, 149.1, 144.1, 131.4, 130.8, 124.9, 123.3, 117.8, 114.7, 111.2, 111.1, 56.1, 56.0, 54.8, 47.3, 46.2; Anal. Calcd for $C_{22}H_{26}N_2O_3$ (366.45): C, 72.11; H, 7.15; N, 7.64, found C, 72.34; H, 7.26; N, 7.88.

3-(4-(4-methylpiperazin-1-yl)phenyl)-1-(3,4,5-trimethoxyphenyl)prop-2-en-1-one **(2L):** Yellow solid: 80% yield; mp 188–190 °C; IR (KBr, cm^{-1}) 3005 (CH aromatic), 2960, 2939 (CH aliphatic), 1647 (C═O), 1566 (C═C); ^{1}H NMR (400 MHz, DMSO-d_6) δ 7.76–7.70 (m, 3H, ArH + CH═CH—CO), 7.67 (d, J = 15.6 Hz, 1H, CH═CH—CO), 7.40 (s, 2H, ArH), 6.98 (d, J = 8.4 Hz, 2H, ArH), 3.90 (s, 6H, 2OCH_3), 3.76 (s, 3H, OCH_3), 3.29 (t, J = 4.8 Hz, 4H, $2CH_2$ piperazine), 2.44 (t, J = 4.8 Hz, 4H, $2CH_2$ piperazine), 2.22 (s, 3H, NCH_3); ^{13}C NMR (100 MHz, DMSO-d_6) δ:188.0, 153.3, 152.9, 144.9, 142.0, 134.0, 131.1, 124.7, 117.8, 114.6, 106.3, 60.6, 56.6, 54.8, 47.2, 46.1; Anal. Calcd for $C_{23}H_{28}N_2O_4$ (396.48) C, 69.67; H, 7.12; N, 7.07, found C, 69.91; H, 7.28; N, 7.29.

4.1.3. General procedure for the preparation of substituted 2H-chromen-2-one chalcone derivatives ***(3a-f)***

A mixture of 3-acetyl-2*H*-chromen-2-one (1.88 g, 0.01 mol) and the selected aldehyde (**1a-f**) were dissolved in 95% ethanol (50 mL). Piperidine (0.085 g, 0.001 mol) was added and the mixture was heated under reflux for 6 h. After cooling the solid product was filtered, washed with ethanol, dried, and crystallized from ethanol.

3-(3-(4-(4-chlorophenoxy)phenyl)acryloyl)–2H-chromen-2-one **(3a):** Orange solid: 61% yield; mp 178–180 °C; IR (KBr, cm^{-1}) 3082 (CH aromatic), 1724, 1678 (2C═O), 1608 (C═C); ^{1}H NMR (400 MHz, DMSO-d_6) δ 8.61 (s, 1H, C4H of chromene), 8.41 (d, J = 8.0 Hz, 1H, ArH), 8.24 (s, 1H, ArH), 7.86 (d, J = 7.6 Hz, 1H, ArH), 7.71 (t, J = 7.6 Hz, 1H, ArH), 7.64 (t, J = 8.0 Hz, 1H, ArH), 7.54–7.41 (m, 6H, ArH), 7.21–7.13 (m, 1H, ArH), 7.05–7.00 (m, 1H, ArH), 6.83–6.75 (m, 1H, ArH); ^{13}C NMR (100 MHz, DMSO-d_6) δ:189.1, 164.4, 161.3, 153.7, 150.7, 143.4, 133.1, 131.5, 129.5, 125.7, 125.2, 124.6, 118.2, 117.8, 116.5, 113.4, 99.9; Anal. Calcd for $C_{24}H_{15}ClO_4$ (402.83): C, 71.56; H,

3.75, found C, 71.38; H, 3.86.

***3-(3-(4-(4-bromophenoxy)phenyl)acryloyl)–2H-chromen-2-one* (3b)**: Orange solid: 60% yield; mp 194–196 °C; IR (KBr, cm^{-1}) 3097 (CH aromatic), 724, 1678 (2C═O), 1608 (C═C); ^{1}H NMR (400 MHz, DMSO-d_6) δ 8.67 (s, 1H, C4H of chromene), 7.95 (dd, J = 1.6, 7.6 Hz, 1H, ArH), 7.82–7.74 (m, 4H, ArH + CH═CH—CO), 7.63–7.57 (m, 3H, ArH + CH═CH—CO), 7.50 (d, J = 8.4 Hz, 1H, ArH), 7.46–7.42 (m, 1H, ArH), 7.12–7.06 (m, 4H, ArH); ^{13}C NMR (100 MHz, DMSO-d_6) δ:187.7, 159.1, 158.8, 155.5, 154.8, 147.2, 143.6, 134.6, 133.4, 131.3, 130.8, 130.3, 126.0, 125.4, 124.3, 121.9, 119.1, 118.8, 116.6, 116.4; Anal. Calcd for $C_{24}H_{15}BrO_4$ (447.28): C, 64.45; H, 3.38;, found C, 64.31; H, 3.49.

***3-(3-(4-(4-methoxyphenoxy)phenyl)acryloyl)–2H-chromen-2-one* (3c)**: Orange solid: 52% yield; mp 140–142 °C; IR (KBr, cm^{-1}) 3097 (CH aromatic), 2958, 2935 (CH aliphatic), 1732, 1654 (2C═O), 1604 (C═C); ^{1}H NMR (400 MHz, DMSO-d_6) δ 8.64 (s, 1H, C4H of chromene), 7.93 (dd, J = 1.6, 7.6 Hz, 1H, ArH), 7.76–7.72 (m, 4H, ArH + CH═CH—CO), 7.55 (d, J = 16.0 Hz, 1H,CH═CH–CO), 7.48 (d, J = 8.4 Hz, 1H, ArH), 7.45–7.41 (m, 1H, ArH), 7.09–7.05 (m, 2H, ArH), 7.02–6.94 (m, 4H, ArH), 3.77 (s, 3H, OCH_3); ^{13}C NMR (100 MHz, DMSO-d_6) δ:187.5, 160.9, 158.8, 156.6, 154.8, 148.7, 147.1, 144.2, 134.5, 131.2, 130.8, 129.1, 126.0, 125.3, 123.7, 121.8, 118.8, 117.5, 116.6, 115.6, 55.8; Anal. Calcd for $C_{25}H_{18}O_5$ (398.41): C, 75.37; H, 4.55, found C, 75.63; H, 4.81.

***3-(3-(4-(piperidin-1-yl)phenyl)acryloyl)–2H-chromen-2-one* (3d)**: Red solid: 52% yield; mp 148–150 °C; IR (KBr, cm^{-1}) 3074 (CH aromatic), 2924, 2846 (CH aliphatic), 1728, 1681 (2C═O), 1600 (C═C); ^{1}H NMR (400 MHz, DMSO-d_6) δ 8.60 (s, 1H, C4H of chromene), 7.92 (dd, J = 1.6, 8.0 Hz, 1H, ArH), 7.75–7.71 (m, 1H, ArH), 7.68 (d, J = 15.6 Hz, 1H, CH═CH—CO), 7.57 (d, J = 8.8 Hz, 2H, ArH), 7.49 7.38 (m, 3H, ArH + CH═CH—CO), 6.95 (d, J = 8.8 Hz, 2H, ArH), 3.44–3.30 (m, 4H, $2CH_2$ piperidine, appeared after D_2O), 1.58 (s, 6H, $3CH_2$ piperidine); ^{13}C NMR (100 MHz, DMSO-d_6) δ:186.8, 158.9, 154.7, 153.2, 146.6, 145.6, 134.3, 131.1, 130.6, 126.3, 125.2, 123.5, 120.0, 118.9, 116.3, 114.5, 48.3, 25.3, 24.4; Anal. Calcd for $C_{23}H_{21}NO_3$ (359.42): C, 76.86; H, 5.89; N, 3.90; found C, 77.23; H, 6.19; N, 3.68;

***3-(3-(4-morpholinophenyl)acryloyl)–2H-chromen-2-one* (3e):** Red solid: 69% yield; mp 180–182 °C; IR (KBr, cm^{-1}) 3093 (CH aromatic), 2980, 2854 (CH aliphatic), 1724, 1651 (2C═O), 1604 (C═C); ^{1}H NMR (400 MHz, DMSO-d_6) δ 8.61 (s, 1H, C4H of chromene), 7.95–7.92 (m, 1H, ArH), 7.76–7.71 (m, 2H, ArH + CH═CH—CO),), 7.68–7.67 (m, 1H, ArH), , 7.59 (d, J = 8.8 Hz, 1H, ArH), 7.50–7.47 (m, 1H, ArH), 7.45–7.42 (m, 1H, ArH), 7.39 (d, J = 15.6 Hz, 1H, CH═CH—CO), 7.00 (d, J = 9.2 Hz, 2H, ArH), 3.74 (t, J = 4.8 Hz, 4H, $2CH_2$ morpholine), 3.27 (t, J = 4.8 Hz, 4H, $2CH_2$ morpholine); ^{13}C NMR (100 MHz, DMSO-d_6) δ:187.1, 158.9, 154.7, 153.2, 146.6, 145.4, 134.3, 130.9, 130.7, 126.3, 125.3, 124.7, 120.9, 118.9, 116.6, 114.5, 66.3, 47.4; Anal. Calcd for $C_{22}H_{19}NO_4$ (361.39): C, 73.12; H, 5.30; N, 3.88; found C, 73.41; H, 5.39; N, 4.15.

***3-(3-(4-(4-methylpiperazin-1-yl)phenyl)acryloyl)–2H-chromen-2-one* (3f):** Red solid: 61% yield; mp 141–143 °C; IR (KBr, cm^{-1}) 3082 (CH aromatic), 2966, 2935 (CH aliphatic), 1720, 1651 (2C═O), 1605 (C═C); ^{1}H NMR (400 MHz, DMSO-d_6) δ 8.61 (s, 1H, C4H of chromene), 7.93 (dd, J = 1.6, 7.6 Hz, 1H, ArH), 7.77–7.72 (m, 1H, ArH) 7.69 (d, J = 15.6 Hz, 1H, CH═CH—CO), 7.61 (d, J = 8.8 Hz, 2H, ArH), 7.54–7.41 (m, 3H, ArH + CH═CH—CO), 6.99 (d, J = 8.4 Hz, 2H, ArH), 3.31 (t, J = 5.2 Hz, 4H, $2CH_2$ piperazine), 2.44 (t, J = 5.2 Hz, 4H, $2CH_2$ piperazine), 2.22 (s, 3H, NCH_3); ^{13}C NMR (100 MHz, DMSO-d_6) δ:187.2, 158.9, 154.7, 153.1, 146.6, 145.6, 134.3, 131.0, 130.7, 126.5, 125.3, 124.2, 120.6, 118.9, 116.6, 114.7, 54.7, 47.1, 46.7; Anal. Calcd for $C_{23}H_{22}N_2O_3$ (374.43): C, 73.78; H, 5.92; N, 7.48, found C, 73.62; H, 6.21; N, 7.67.

4.2. Biology

4.2.1. Cell culture

RAW264.7 (murine macrophage cells) was obtained from the American Tissue Culture Collection (Manassas, VA, USA). The cells were cultured in DMEM supplemented with 10% FBS, and 1% penicillin–streptomycin (PAA Laboratories GmbH, PA, Austria with 5% CO_2 at 37 °C.

4.2.2. NO assay

RAW264.7 cells were pretreated with the target compounds at above-mentioned concentrations for 2 h and treated with LPS (1 μg/mL) for 24 h. To measure the NO in the culture medium, 100 L of Griess reagent (Sigma-Aldrich, St. Louis, MO, USA) was added to 100 L of the culture medium and incubated at room temperature for 10 min. The optical density (OD) at 540 nm was examined with the ELISA reader (Molecular Devices, Silicon Valley, CA, USA) [44].

4.2.3. Cell viability assay

RAW264.7 cells were treated with **2f** at mentioned concentrations for 24 h. The 100 μL of fresh medium was exchanged and 10 L WST-1® (Daeil Lab service, Seoul, Korea) was added into each well. After 3 h, the OD was measured with the ELISA reader at 460 nm [44].

4.2.4. Western blot analysis

RAW264.7 cells were collected and lysed with an ice-cold lysis buffer. Aliquots from each sample were separated by 12% SDS-polyacrylamide gel electrophoresis and transferred to a nitrocellulose membrane (PALL Life Sciences, Pensacola, MI, USA). The membrane was blocked with 5% skim milk in phosphate buffered saline tween-20 (PBST) buffer for 1 h. After blocking, the membrane was incubated with each of the primary antibodies, which were diluted 1:1000 with 5% BSA in 1x-PBST at 4 °C overnight. The blots were washed three times with PBST buffer, and the membrane was incubated with HRP-conjugated second antibodies (anti-rabbit IgG and anti-mouse IgG, diluted 1:2000 with 5% skim milk in 1xPBST) at room temperature for 1 h. The blots were washed three times using PBST buffer and detected by an ECL solution® (AbFontier, Gyeonggi, Korea) [44].

4.2.5. Statistic analysis

All the experiments were executed in triplicate and the results are expressed as the means ± standard errors of the mean (SEM).

4.3. Molecular docking

The X-ray crystallographic structure of Human IκB kinase beta (PDB ID: 4KIK) was obtained from the protein data bank available at the RCSB Protein Data Bank, (http://www.pdb.org) with 2.83 Å resolution. All the molecular modeling studies were carried out using Molecular Operating Environment (MOE 2014.09; Chemical Computing Group, Canada) as the computational software. Hydrogen atoms were added, and the protonation states of the amino acid residues were assigned using the Protonate 3D algorithm. Compound **2f** were modelled using MOE builder, and the structure was energy minimized using the MMFF94x force field. Docking studies of our synthesized compound into the active site was done by using the MOE Dock tool and the final docked complexes of ligand–enzyme was selected according to the criteria of interaction energy combined with geometrical matching quality.

Declaration of Competing Interest

The authors declare that they have no known competing financial interests or personal relationships that could have appeared to influence the work reported in this paper.

Appendix A. Supplementary material

Supplementary data to this article can be found online at https://doi.org/10.1016/j.bioorg.2021.104630.

References

[1] A. Mantovani, P. Allavena, A. Sica, F. Balkwill, Cancer-related inflammation, Nature 454 (7203) (2008) 436–444.
[2] K. Seibert, J.L. Masferrer, Role of inducible cyclooxygenase (COX-2) in inflammation, Receptor 4 (1) (1994) 17–23.
[3] P. Rao, E.E. Knaus, Evolution of nonsteroidal anti-inflammatory drugs (NSAIDs): cyclooxygenase (COX) inhibition and beyond, J. Pharm. Pharm. Sci. 11 (2) (2008) 81s–110s.
[4] Y. Jiang, K.P. Rakesh, N.S. Alharbi, H.K. Vivek, H.M. Manukumar, Y.H. E. Mohammed, H.-L. Qin, Radical scavenging and anti-inflammatory activities of (hetero)arylethenesulfonyl fluorides: Synthesis and structure-activity relationship (SAR) and QSAR studies, Bioorg. Chem. 89 (2019) 103015.
[5] C.S. Karthik, H.M. Manukumar, A.P. Ananda, S. Nagashree, K.P. Rakesh, L. Mallesha, H.-L. Qin, S. Umesha, P. Mallu, N.B. Krishnamurthy, Synthesis of novel benzodioxane midst piperazine moiety decorated chitosan silver nanoparticle against biohazard pathogens and as potential anti-inflammatory candidate: A molecular docking studies, Int. J. Biol. Macromol. 108 (2018) 489–502.
[6] S.-M. Wang, G.-F. Zha, K. Rakesh, N. Darshini, T. Shubhavathi, H. Vivek, N. Mallesha, H.-L. Qin, Synthesis of benzo [d] thiazole-hydrazone analogues: molecular docking and SAR studies of potential H+/K+ ATPase inhibitors and anti-inflammatory agents, MedChemComm 8 (6) (2017) 1173–1189.
[7] X. Chen, J. Leng, K. Rakesh, N. Darshini, T. Shubhavathi, H. Vivek, N. Mallesha, H.-L. Qin, Synthesis and molecular docking studies of xanthone attached amino acids as potential antimicrobial and anti-inflammatory agents, MedChemComm 8 (8) (2017) 1706–1719.
[8] C. Li, M.B. Sridhara, K.P. Rakesh, H.K. Vivek, H.M. Manukumar, C.S. Shantharam, H.-L. Qin, Multi-targeted dihydrazones as potent biotherapeutics, Bioorg. Chem. 81 (2018) 389–395.
[9] T. Liu, L. Zhang, D. Joo, S.-C. Sun, NF-κB signaling in inflammation, Signal Transduct Target Ther 2 (2017) 17023.
[10] J.N. Sharma, A. Al-Omran, S.S. Parvathy, Role of nitric oxide in inflammatory diseases, Inflammopharmacology 15 (6) (2007) 252–259.
[11] Z. Rozmer, P. Perjési, Naturally occurring chalcones and their biological activities, Phytochem. Rev. 15 (1) (2016) 87–120.
[12] B. Srinivasan, T.E. Johnson, R. Lad, C. Xing, Structure-activity relationship studies of chalcone leading to 3-hydroxy-4,3',4',5'-tetramethoxychalcone and its analogues as potent nuclear factor kappaB inhibitors and their anticancer activities, J. Med. Chem. 52 (22) (2009) 7228–7235.
[13] D.K. Mahapatra, S.K. Bharti, V. Asati, Anti-cancer chalcones: Structural and molecular target perspectives, Eur. J. Med. Chem. 98 (2015) 69–114.
[14] S. Acharjee, T.K. Maity, S. Samanta, S. Mana, T. Chakraborty, T. Singha, A. Mondal, Antihyperglycemic activity of chalcone based novel 1-{3-[3-(substituted phenyl) prop-2-enoyl] phenyl} thioureas, Synth. Commun. 48 (23) (2018) 3015–3024.
[15] M. Xu, P. Wu, F. Shen, J. Ji, K.P. Rakesh, Chalcone derivatives and their antibacterial activities: Current development, Bioorg. Chem. 91 (2019) 103133.
[16] J. Wu, J. Li, Y. Cai, Y. Pan, F. Ye, Y. Zhang, Y. Zhao, S. Yang, X. Li, G. Liang, Evaluation and discovery of novel synthetic chalcone derivatives as anti-inflammatory agents, J. Med. Chem. 54 (23) (2011) 8110–8123.
[17] S. Vogel, M. Barbic, G. Jürgenliemk, J. Heilmann, Synthesis, cytotoxicity, anti-oxidative and anti-inflammatory activity of chalcones and influence of A-ring modifications on the pharmacological effect, Eur. J. Med. Chem. 45 (6) (2010) 2206–2213.
[18] Z. Nowakowska, A review of anti-infective and anti-inflammatory chalcones, Eur. J. Med. Chem. 42 (2) (2007) 125–137.
[19] P. Lorenzo, R. Alvarez, M.A. Ortiz, S. Alvarez, F.J. Piedrafita, Á.R. de Lera, Inhibition of IκB kinase-β and anticancer activities of novel chalcone adamantyl arotinoids, J. Med. Chem. 51 (17) (2008) 5431–5440.
[20] Y. Yang, Z. Wei, A.T. Teichmann, F.H. Wieland, A. Wang, X. Lei, Y. Zhu, J. Yin, T. Fan, L. Zhou, C. Wang, L. Chen, Development of a novel nitric oxide (NO) production inhibitor with potential therapeutic effect on chronic inflammation, Eur. J. Med. Chem. 193 (2020) 112216.
[21] X. Xie, J. Tu, H. You, B. Hu, Design, synthesis, and biological evaluation of novel EF24 and EF31 analogs as potential IκB kinase β inhibitors for the treatment of pancreatic cancer, Drug Des. Devel. Ther. 11 (2017) 1439–1451.
[22] Y. Zhang, J. Wu, S. Ying, G. Chen, B. Wu, T. Xu, Z. Liu, X. Liu, L. Huang, X. Shan, Y. Dai, G. Liang, Discovery of new MD2 inhibitor from chalcone derivatives with anti-inflammatory effects in LPS-induced acute lung injury, Sci. Rep. 6 (1) (2016) 25130.
[23] H. ur Rashid, Y. Xu, N. Ahmad, Y. Muhammad, L. Wang, Promising anti-inflammatory effects of chalcones via inhibition of cyclooxygenase, prostaglandin E2, inducible NO synthase and nuclear factor κb activities, Bioorg. Chem. 87 (2019) 335–365.
[24] N. Chainani-Wu, Safety and anti-inflammatory activity of curcumin: A component of tumeric (curcuma longa), J. Alternat. Complement. Med. 9 (1) (2003) 161–168.
[25] D.J. Hadjipavlou-Litina, K.E. Litinas, C. Kontogiorgis, The anti-inflammatory effect of coumarin and its derivatives, Antiinflamm. Antiallergy Agents Med. Chem. 6 (4) (2007) 293–306.
[26] J. Grover, S.M. Jachak, Coumarins as privileged scaffold for anti-inflammatory drug development, RSC Adv. 5 (49) (2015) 38892–38905.
[27] H.-L. Qin, Z.-W. Zhang, L. Ravindar, K.P. Rakesh, Antibacterial activities with the structure-activity relationship of coumarin derivatives, Eur. J. Med. Chem. 207 (2020) 112832.
[28] H.M. Revankar, S.N.A. Bukhari, G.B. Kumar, H.-L. Qin, Coumarins scaffolds as COX inhibitors, Bioorg. Chem. 71 (2017) 146–159.
[29] C.S. Lino, M.L. Taveira, G.S.B. Viana, F.J.A. Matos, Analgesic and antiinflammatory activities of Justicia pectoralis Jacq and its main constituents: coumarin and umbelliferone, Phytother. Res. 11 (3) (1997) 211–215.
[30] O.A. Nurkenov, S.D. Fazylov, A.E. Arinova, K.M. Turdybekov, D.M. Turdybekov, S. A. Talipov, B.T. Ibragimov, Synthesis, structure and chemical transformations of 4-aminobenzaldehyde, Russ. J. Gen. Chem. 83 (10) (2013) 1864–1868.
[31] M. Mahdavi, S. Mohammadi-Izad, M. Saeedi, M. Safavi, S.E.S. Ebrahimi, A. Foroumadi, A. Shafiee, Synthesis and cytotoxicity of novel chromenone derivatives bearing 4-nitrophenoxy phenyl acryloyl moiety, J. Iran. Chem. Soc. 13 (6) (2016) 1139–1144.
[32] O.O. Ajani, R.I. Ituen, A. Falomo, Facile synthesis and characterization of substituted pyrimidin-2 (1H)-ones and their chalcone precursors, Pakistan J. Sci. Ind. Res. Series A: Phys. Sci. 54 (2) (2011) 59–67.
[33] C. Anwar, Y.D. Prasetyo, S. Matsjeh, W. Haryadi, E.N. Sholikhah, N. Nendrowati, Synthesis of chalcone derivatives and their in vitro anticancer test against breast (T47D) and colon (WiDr) cancer cell line, Indones. J. Chem. 18 (1) (2018) 102–107.
[34] O.O. Ajani, O. Ajayi, J.A. Adekoya, T.F. Owoeye, B.M. Durodola, O.M. Ogunleye, Comparative study of microwave-assisted and conventional synthesis of 3-[1-(s-phenylimino) ethyl]-2H-chromen-2-ones and selected hydrazone derivatives, J. Appl. Sci. 16 (3) (2016) 77–87.
[35] Y.R. Prasad, P.R. Kumar, C.A. Deepti, M.V. Ramana, Synthesis and antimicrobial activity of some novel chalcones of 2-hydroxy-1-acetonapthone and 3-acetyl coumarin, J. Chem. 3 (4) (2006) 236–241.
[36] N.S. Kirkby, M.V. Chan, A.K. Zaiss, E. Garcia-Vaz, J. Jiao, L.M. Berglund, E. F. Verdu, B. Ahmetaj-Shala, J.L. Wallace, H.R. Herschman, M.F. Gomez, J. A. Mitchell, Systematic study of constitutive cyclooxygenase-2 expression: Role of NF-κB and NFAT transcriptional pathways, Proc. Natl. Acad. Sci. USA 113 (2) (2016) 434–439.
[37] N.S. Kirkby, M.H. Lundberg, L.S. Harrington, P.D.M. Leadbeater, G.L. Milne, C. M. Potter, M. Al-Yamani, O. Adeyemi, T.D. Warner, J.A. Mitchell, Cyclooxygenase-1, not cyclooxygenase-2, is responsible for physiological production of prostacyclin in the cardiovascular system, Proc. Natl. Acad. Sci. U S A 109 (43) (2012) 17597–17602.
[38] R. Korhonen, A. Lahti, H. Kankaanranta, E. Moilanen, Nitric oxide production and signaling in inflammation, Curr. Drug Targets Inflamm. Allergy 4 (4) (2005) 471–479.
[39] G. Nagy, A. Koncz, T. Telarico, D. Fernandez, B. Ersek, E. Buzás, A. Perl, Central role of nitric oxide in the pathogenesis of rheumatoid arthritis and systemic lupus erythematosus, Arthritis Res. Ther. 12 (3) (2010), 210–210.
[40] N.S. Bryan, M.B. Grisham, Methods to detect nitric oxide and its metabolites in biological samples, Free Radic. Biol. Med. 43 (5) (2007) 645–657.
[41] J.C. Stockert, R.W. Horobin, L.L. Colombo, A. Blázquez-Castro, Tetrazolium salts and formazan products in Cell Biology: Viability assessment, fluorescence imaging, and labeling perspectives, Acta Histochem. 120 (3) (2018) 159–167.
[42] K.R. Manjeet, B. Ghosh, Quercetin inhibits LPS-induced nitric oxide and tumor necrosis factor-alpha production in murine macrophages, Int. J. Immunopharmacol 21 (7) (1999) 435–443.
[43] A. Daikonya, S. Katsuki, S. Kitanaka, Antiallergic agents from natural sources 9. Inhibition of nitric oxide production by novel chalcone derivatives from mallotus philippinensis (euphorbiaceae), Chem. Pharm. Bull. 52 (11) (2004) 1326–1329.
[44] D. Hwang, B.W. Son, P.G. Shin, J.S. Choi, Y.B. Seo, G.D. Kim, Toluhydroquinone from Aspergillus sp. suppress inflammatory mediators via nuclear factor-κB and mitogen-activated protein kinases pathways in lipopolysaccharide-induced RAW264.7 cells, J. Pharm. Pharmacol. 67 (9) (2015) 1297–1305.
[45] P.P. Tak, G.S. Firestein, NF-κB: a key role in inflammatory diseases, J. Clin. Investig. 107 (1) (2001) 7–11.
[46] T. Kawai, S. Akira, Signaling to NF-kappaB by Toll-like receptors, Trends Mol. Med. 13 (11) (2007) 460–469.
[47] S. Liu, Y.R. Misquitta, A. Olland, M.A. Johnson, K.S. Kelleher, R. Kriz, L.L. Lin, M. Stahl, L. Mosyak, Crystal structure of a human IκB kinase β asymmetric dimer, J. Biol. Chem. 288 (31) (2013) 22758–22767.
[48] G. Chen, L. Jiang, L. Dong, Z. Wang, F. Xu, T. Ding, L. Fu, Q. Fang, Z. Liu, X. Shan, G. Liang, Synthesis and biological evaluation of novel indole-2-one and 7-aza-2-oxindole derivatives as anti-inflammatory agents, Drug Des. Devel. Ther. 8 (2014) 1869–1892.
[49] E. Polo, N. Ibarra-Arellano, L. Prent-Peñaloza, A. Morales-Bayuelo, J. Henao, A. Galdámez, M. Gutiérrez, Ultrasound-assisted synthesis of novel chalcone, heterochalcone and bis-chalcone derivatives and the evaluation of their antioxidant properties and as acetylcholinesterase inhibitors, Bioorg. Chem. 90 (2019) 103034.
[50] B. Zhou, P. Jiang, J. Lu, C. Xing, Characterization of the fluorescence properties of 4-dialkylaminochalcones and investigation of the cytotoxic mechanism of chalcones, Arch. Pharm. 349 (7) (2016) 539–552.